A00-39775 AIAA-2000-4033

Automated Design of Low-Thrust Gravity-Assist Trajectories

Anastassios E. Petropoulos* and James M. Longuski†
School of Aeronautics and Astronautics, Purdue University,
West Lafayette, Indiana 47907-1282

The promise of low-thrust gravity-assist (LTGA) trajectories is considerable because they can grant access to scientific targets for low propellant costs and with short flight times. Low-thrust propulsion systems have already been demonstrated. Coupling this technology with the proven gravity-assist technique promises to open doors for future missions to distant targets. We introduce a new software tool which automatically searches for LTGA trajectories over a wide range of launch energies, launch dates, and thruster characteristics. The algorithm relies on the theory of shape-based trajectory design, developed earlier. We use the tool to study missions to Mercury (via gravity assist from Venus), to Ceres (via gravity assist from Mars), and to Tempel 1. Our broad design searches confirm the likelihood of low-cost trajectories for launch dates corresponding to optimal trajectories in the literature.

Introduction

We describe a shape-based theory, and its incorporation into computer software, that provides a broad search capability for low-thrust trajectories including gravity assists at multiple bodies. For conic trajectories with impulsive ΔVs, this broad search capability is already provided by STOUR (the Satellite Tour Design Program[1-5]). Considering STOUR's success, an obvious extension of its capability is the inclusion of low-thrust arcs, which can capitalize on highly efficient propulsion techniques, such as solar electric ion propulsion (*e.g.* the NSTAR thruster on the *Deep Space 1* mission[6]).

The literature on low-thrust, gravity-assist (LTGA) trajectory design, concentrates on the problem of (single-point) trajectory optimization. In this paper, we concentrate on automated design, allowing broad searches over various key trajectory parameters such as launch date, launch energy, time of flight, and propellant fraction. Analytic solutions to the two-body equations of motion are known for only highly specialized cases in the LTGA problem. For example, by assuming tangential thrust inversely proportional to $r\cos\gamma$ (where γ is the flight path angle), Markopoulos[7] obtains radius as an explicit function of polar angle. In contrast, we take a heuristic approach, wherein a trajectory shape is itself directly assumed, with the required thrust computed *a posteriori*. Explicit analytic expressions for the shape allow rapid computation of trajectory arcs and easy coupling with gravity assists. The results should be useful not only as aids to LTGA mission designers, but also as starting guesses for single-point trajectory optimization, particularly with direct methods.[8-10]

By making a wise choice for the type of shape to use, only a few shape parameters will be needed to obtain a variety of realistic trajectory arcs, thus reducing the number of computations needed to determine an arc, given certain conditions. After examining a number of shapes,[11] we selected the "exponential sinusoid," given in polar coordinates by

$$r = k_0 e^{q\theta + k_1 \sin(k_2\theta + \phi)} \tag{1}$$

where the k_i, q, and ϕ are constant parameters. The parameter q is taken here as zero, since non-zero values are often detrimental to the performance of the trajectory arcs. As explained in Ref. 11, for several shapes, the exponential sinusoid included, specifying an arbitrary thrust profile typically will require the solution of two coupled, intractable differential equations to obtain the velocity at any point on the shape and the time of flight over an arc. On the other hand, if tangential thrust is specified, *i.e.* thrust along or against the velocity vector, then the time of flight is available through a simple quadrature, and the velocity and thrust magnitude are explicitly available analytically. We first describe the computational implementation of the shape-based approach, and then present results obtained with this STOUR-LTGA software.

*Doctoral Candidate, Member AIAA, Student Member AAS.

†Professor, Associate Fellow AIAA, Member AAS.

Methodology

The motion of the spacecraft between bodies (i.e. on each leg) is considered in two separate parts, the in-plane motion and the out-of-plane motion. The in-plane motion is assumed to follow an exponential sinusoid, Eq. 1, with tangential thrust and $q = 0$. The time rate of change of the polar angle is then given by:[11]

$$\dot{\theta}^2 = \left(\frac{\mu}{r^3}\right) \frac{1}{\tan^2\gamma + k_1 k_2^2 s + 1} \tag{2}$$

where μ is the gravitational parameter of the central body and $s \equiv \sin(k_2\theta + \phi)$. In addition, the thrust acceleration magnitude is determined by the shape parameters and the location on the curve:[11]

$$a \equiv \frac{F}{\mu/r^2} = \frac{|\tan\gamma|}{2\cos\gamma}\left[\frac{1}{\tan^2\gamma + k_1 k_2^2 s + 1} - \frac{k_2^2(1 - 2k_1 s)}{(\tan^2\gamma + k_1 k_2^2 s + 1)^2}\right] \tag{3}$$

where F is the thrust acceleration, and a is its non-dimensional value in local solar g's. The shape and tangential thrust assumptions require thrust along the velocity vector for positive flight path angles and against it for negative flight path angles.

The out-of-plane motion is based on an analysis of the orbital angular momentum vector, where the out-of-plane angle and speed are approximated from the in-plane angular momentum and velocity components. The approximations are increasingly better the smaller the out-of-plane angles.

In-plane motion

The program steps through the launch dates and launch v_∞s specified by the user, and for each computes trajectories that reach the next body. The launch v_∞ vector is assumed to lie in the body's orbit plane, pointing in any direction. In the case of a flyby, a B-Plane angle[12] of 0° or 180° is assumed, and the v_∞ turn angle is constrained by altitude. The low-thrust reference plane (*i.e.* where the planar motion occurs) for the next leg is taken as normal to the spacecraft's initial angular momentum vector. The program steps through the full range of in-plane orientations for the outgoing v_∞ vector. For each outgoing v_∞ vector, there corresponds a heliocentric flight path angle and speed; hence, from the geometry of the shape and the dynamics (Eqs. 1 and 2), the quantity $k_{12s} \equiv k_1 k_2^2 s$ can be determined, resulting in the constraint relationship

$$k_1^2 k_2^4 - k_2^2 \tan^2\gamma - k_{12s}^2 = 0 \tag{4}$$

There then remains one free shape parameter, taken as k_2, which is used to effect the targeting of the next body. The search over k_2 for exponential sinusoids meeting the target body is narrowed in several ways. Without loss of generality, only positive values are considered for k_1 and k_2. To avoid singularities around periapsis, we require

$$1 - k_1 k_2^2 > 0 \tag{5}$$

which ensures that the denominator in Eq. 2 is always positive (when zero or negative, the exponential sinusoid cannot be followed using tangential thrust). For practical purposes, upper limits of one and two are imposed on k_2 and k_1, respectively, since the required thrust levels become untenably high when $(1 - k_1 k_2^2)$ approaches zero. Furthermore, if only one parameter is large and the other very small, the thrust levels may be acceptable, but the trajectory shape will not be useful. Lastly, a range of k_2 values can be determined for which the resulting exponential sinusoid will intersect the projection onto the low-thrust reference plane of the target body's orbit. For outbound targets, *i.e.*, those whose minimum projected radius, $\rho_{\min}$, is greater than the current radius, r_B, we obtain after some algebraic manipulations based on Eqs. 1 and 4:

$$k_2^2 \le \frac{\tan^2\gamma - 2k_{12s}\ln(\rho_{\min}/r_B)}{[\ln(\rho_{\min}/r_B)]^2} \tag{6}$$

For inbound targets, *i.e.*, those whose maximum projected radius, $\rho_{\max}$, is greater than the current radius, we similarly obtain

$$k_2^2 \le \frac{\tan^2\gamma + 2k_{12s}\ln(r_B/\rho_{\max})}{[\ln(r_B/\rho_{\max})]^2} \tag{7}$$

For all other targets, no additional constraints can be imposed on k_2.

Thus, for each turn angle we establish a range of k_2 values which yield intersections of the exponential sinusoid and the projected orbit of the target. All that remains is to solve for the specific value of k_2, if any, which yields the correct time of flight to the intersection. This is done by stepping through the range of values, and at each step computing the location of the intersection point. No analytic solution being available, this is computed using a step-size and search-direction controlled Newton method, with a suitable initial guess. The time of flight to the intersection is then computed by quadrature, allowing a miss angle to be found — that is, the spacecraft-sun-target angle when the spacecraft reaches the intersection point (with the target projected onto the plane). Thus, we search for a zero miss angle in the

turn angle - k_2 space. There is a one-dimensional continuum of such solutions, which we sample at intervals according to the turn angle and k_2 step sizes. Of course, each exponential sinusoid will usually intersect the target's orbit more than once. We only keep track of the first outbound intersection and the first inbound intersection.

Out-of-plane motion

The target's out-of-plane position at the time of the in-plane encounter is matched by an additional thrust acting along or against the spacecraft's angular momentum vector for some final portion of the transfer arc. This thrust acceleration, denoted f_h, is upwards for above-the-plane targets and downwards otherwise, and is assumed proportional to the inverse-square radius:

$$f_h = a_{0P}\frac{\mu}{r^2}$$

where a_{0P} is a (positive or negative) constant, and the positive f_h direction is taken to be along the angular momentum vector. Since both the in- and out-of-plane thrust will be much smaller than the gravitational attraction of the central body, the in-plane components of the angular momentum, h_x and h_y, behave according to

$$\frac{\mathrm{d}h_x}{\mathrm{d}\theta} \approx \frac{r f_h \sin\theta}{\dot\theta} \quad (8)$$

$$\frac{\mathrm{d}h_y}{\mathrm{d}\theta} \approx -\frac{r f_h \cos\theta}{\dot\theta} \quad (9)$$

where the x direction is taken as lying along $\theta = 0$. We note that to first order, the in-plane thrust does not affect the in-plane angular momentum components. Now, h_x and h_y remain small, so that the total angular momentum is approximately equal to just the out-of-plane component. Thus, at the end of an out-of-plane thrust arc from θ_0 to θ_f, the out-of-plane angle, ϕ, and the speed normal to the plane, v_z, are given by

$$\tan\phi \approx a_{0P}\frac{\mu}{r_f^2\dot\theta_f}\left(I_y \sin\theta_f - I_x\cos\theta_f\right) \quad (10)$$

$$v_z \approx -a_{0P}\frac{\mu}{r_f}\left(I_y \sin\theta_f + I_x\cos\theta_f\right) \quad (11)$$

where subscript f denotes quantities at θ_f, and

$$I_y = \int_{\theta_0}^{\theta_f}\frac{\cos\theta}{r\dot\theta}\mathrm{d}\theta, \quad I_x = \int_{\theta_0}^{\theta_f}\frac{\sin\theta}{r\dot\theta}\mathrm{d}\theta$$

Since the integrals in Eq. 10 must be computed numerically, they are evaluated backwards from the in-plane intersection with the target, to permit, at each integration step, the computation of the a_{0P} required to match the target's out-of-plane angle. The smallest a_{0P} is then kept. The effect of the out-of-plane motion on the time of flight is ignored. This approximate method permits rapid computations, and is increasingly accurate for smaller out-of-plane excursions. While this method is incorporated into STOUR-LTGA, we generally give little consideration to the out-of-plane thrust and associated propellant, since, other than the simple selection of the lowest a_{0P}, this method was developed with regard neither for attaining the most satisfactory thrust profile nor for the benefits to be had by using different B-plane angles.

Propellant consumption

An estimate of the propellant consumption is made by assuming a constant specific impulse (I_{sp}) for the low-thrust engines. This simplification permits the required propellant mass to be expressed as a fraction of the initial spacecraft mass. In addition, we compute separately the propellant fractions required for the in-plane and out-of-plane thrust; from these is then computed a single fraction. Since our approach controls directly only the shape of the trajectory, the required thrust may fall outside the range of more accurate thruster models, such as those used by Sauer.[13] This fact, together with the additional computational burden required by the more accurate thruster models, prompt the constant I_{sp} assumption. The more sophisticated models can be employed in the optimization of specific trajectories selected from the broad searches permitted by our method.

Leg selection

At any body, with a given incoming trajectory, there exists for the next leg a whole continuum of trajectory solutions in the turn-angle - k_2 space. The computational approach samples this continuum at intervals. From each of these sampled solutions, there again arises a continuum of solutions to the next body. Thus, we limit the selection of solutions based on various criteria, to avoid an exponential increase in the number of trajectories that reach the final body. Solutions for a given leg are stored and propagated if, for example, they have the lowest time of flight, the lowest propellant mass fraction, the lowest thrust levels, the lowest arrival v_∞, the highest arrival v_∞, and so on. Currently, the program uses eighteen criteria, which can be activated or deactivated individually for each leg.

Results

We present results from our method for three rendezvous missions. While our method is also applicable to other missions, we specifically chose rendezvous problems due to their difficulty — matching the state of a final body is more challenging than the less-constrained simple flyby or energetic escape. In all cases, the exponential sinusoid shape assumption is used for all the trajectory legs, and launch is from the Earth (E). The first mission is to Mercury (Y) using a gravity assist at Venus (V). The second mission is to the asteroid Ceres (C) via a gravity assist from Mars (M). The third mission is to the comet Tempel 1 (T), without any gravity assist. For ease of reference, Table 1 lists the semimajor axis, eccentricity, and inclination for the heliocentric orbit of each body.

Table 1 Orbital elements for selected bodies

Body	a (AU)	e	i
Mercury	0.39	0.206	7.0°
Venus	0.72	0.007	3.4°
Earth	1.00	0.017	0.0°
Mars	1.52	0.093	1.8°
Ceres	2.77	0.077	10.6°
Tempel 1	3.12	0.517	10.5°

Earth - Venus - Mercury

A broad, preliminary search is first performed over launch dates spaced two days apart between 2002 and 2005, inclusive. Being just a preliminary search to identify candidate launch dates, only two launch v_∞s, of 2.2 km/s and 2.3 km/s, are considered. The time of flight (TOF) to Venus is constrained to be under one Venus year (224.7 days), while the remaining flight time to Mercury is essentially unconstrained. No constraints are imposed on the thrust profile. Figure 1 shows the ecliptic component of the arrival v_∞ at Mercury plotted against launch date for trajectories with a total propellant fraction below 0.45 (only v_∞s less than 15 km/s are shown). Each symbol on the plot corresponds to a trajectory reaching Mercury. The families of trajectories occur roughly every Earth-Venus synodic period (1.6 years) because of the TOF constraint on the EV leg. Allowing, for example, two Venus years on the EV leg broadens the families to the point of merging.

The first family in Fig. 1 straddles the August 27, 2002 launch date of an optimized, low-thrust, EVY rendezvous trajectory reported by Sauer.[13] Thus we perform a more refined and constrained search over launch dates between April and October 2002, inclusive. The launch v_∞ ranges from 1.75 km/s to 2.5 km/s with a step size of 0.25 km/s. The maximum permitted arrival v_∞ is 10 km/s. The thrust acceleration averaged over polar angle is not allowed to exceed 0.5 mm/s^2 for any leg. The maximum thrust acceleration permitted at any point on the trajectory is 1 mm/s^2. As noted by Sauer,[13] the number of revolutions performed by the spacecraft around the sun on the VY leg is sensitive to the thrust capabilities of the propulsion system. Thus, for this refined search, we present in Figs. 2-4 several quantities plotted against spacecraft revolutions for the VY leg. In Fig. 2 we see the expected trend towards lower average thrust accelerations on the VY leg as the number of revolutions increases. (The discrete levels of thrust acceleration are an artifact of the reporting accuracy in the program's output files.) The in-plane propellant mass fraction for the entire trajectory, shown in Fig. 3 which assumes an optimistic I_{sp} of 4095 seconds, generally increases with more revolutions, as anticipated. Similarly, the time of flight for the VY leg also increases, as shown in Fig. 4. The increasing spread in TOF as the number of revolutions increases beyond about four, arises because, to meet the constraints imposed on the search, more and more of the VY legs must pass through apoapsis, which means that their time of flight can be more drastically affected by slight changes in the Venus flyby conditions. Since the spacecraft kinetic energy and potential energy on an exponential sinusoid are symmetric about each apse, passage through apoapsis on the VY leg is useful only in effecting the correct timing for a Mercury encounter. As the thrust at the apses is zero, the briefer the period prior to passage through the apse, the smaller the impact on the propellant consumption.

The arrival v_∞s in this more refined and constrained search are all above about 5 km/s. For the more spiraling trajectories (greater number of revolutions on the VY leg) this is due to the fact that the speed and flight path angle on the exponential sinusoid are close to the values for a circular orbit at the local radius. Thus, given the large eccentricity of Mercury's orbit (see Table 1), an arrival v_∞ of this magnitude is not unexpected. For the less spiraling VY legs, while greater flight path angles can be obtained, the constraints on the thrust do not permit a good match to Mercury's speed. Additional searches show that permitting average thrust accelerations as high as about 0.9 mm/s^2 reduces the ecliptic arrival v_∞ to about 0.6 km/s, with about 1.3 revolutions on the VY leg and an in-plane propellant mass fraction of about 0.35.

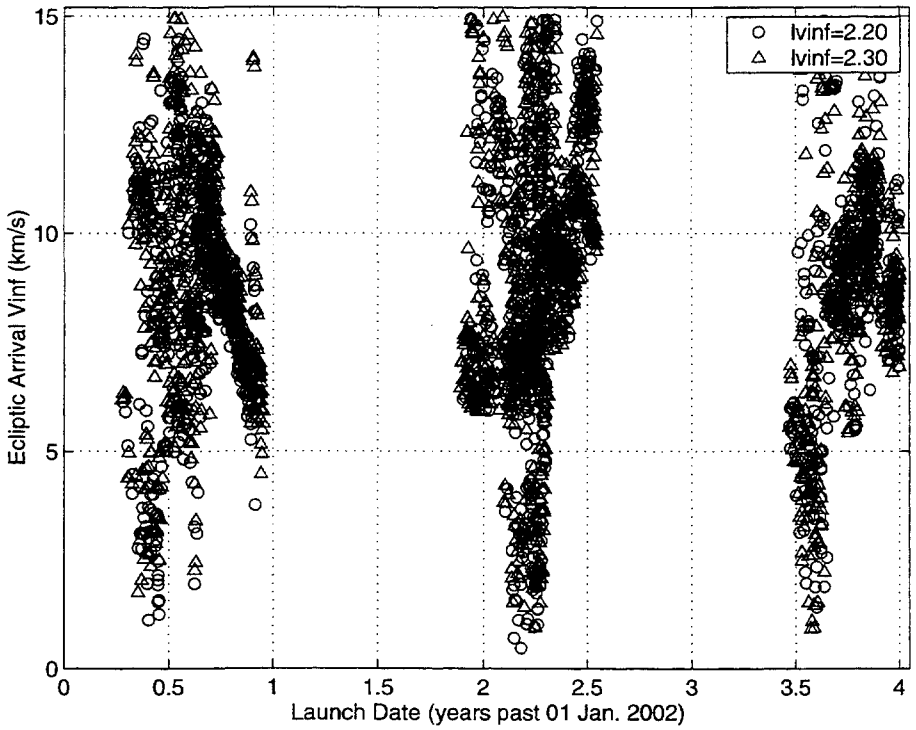

Fig. 1 Broad 4-year search for Earth-Venus-Mercury trajectories.

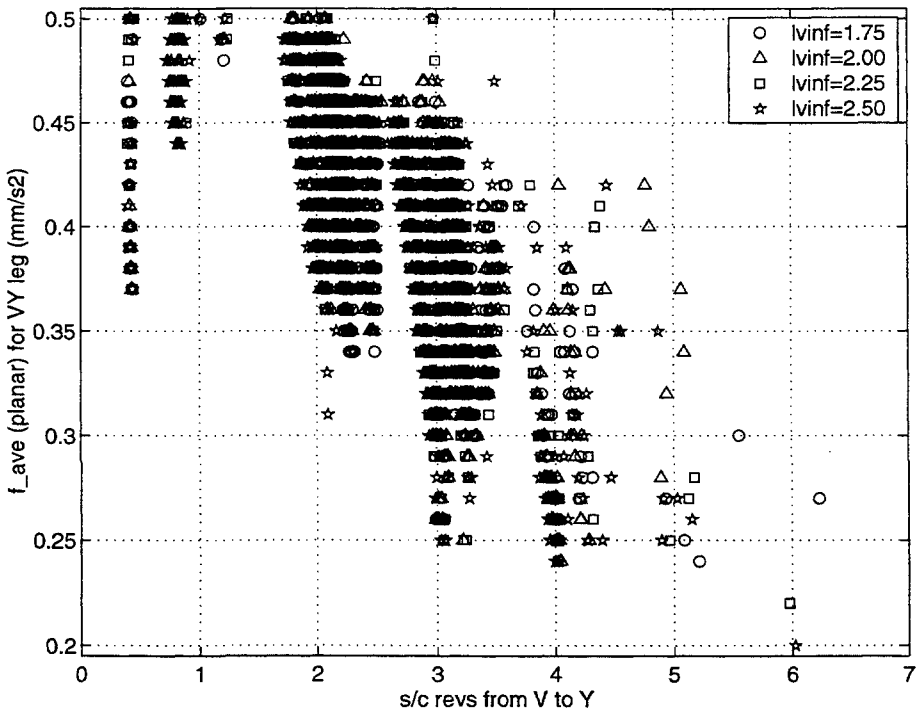

Fig. 2 Average thrust acceleration from Venus to Mercury for Earth-Venus-Mercury trajectories launching between April and October 2002.

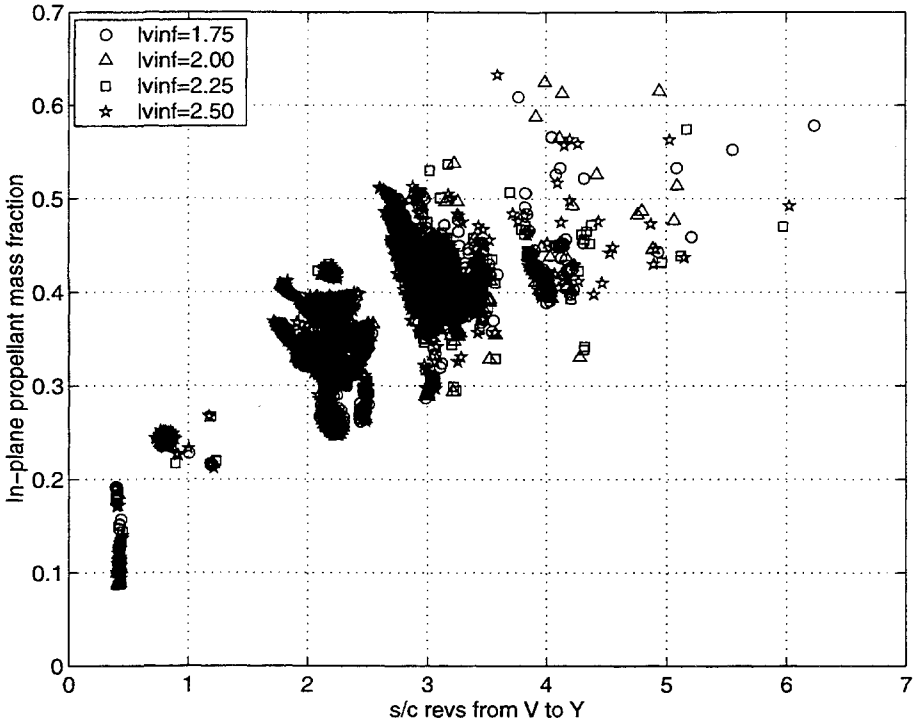

Fig. 3 In-plane propellant consumption for both legs combined of Earth-Venus-Mercury trajectories launching between April and October 2002.

Thus, perhaps more important than achieving zero arrival v_∞, is the selection of trajectories with many revolutions and with thrust levels closer to those attainable in practice. (For example, the NSTAR thruster used by Sauer[13] in his analyses produces a maximum thrust of about 90 mN, which, when acting on a spacecraft mass of 350 kg, provides an acceleration of 0.26 mm/s^2.) The EV leg will typically have smaller thrust levels than the VY leg. Thus, in selecting a trajectory from the refined search, we look for low average thrust accelerations, many revolutions, small propellant fractions, and brief flight times on the VY leg.

Immediately striking in Figs. 3 and 4 is the small trajectory grouping at about 4.3 revolutions with a VY flight time of about 550 days and an in-plane propellant fraction of about 0.34. A more complete searching of the data files confirms this grouping as a good selection. Perhaps the most attractive of the trajectories in the group is the following (for comparison, Sauer's optimized trajectory data are shown in parentheses): Launch on July 30, 2002 (August 27, 2002) with a v_∞ of 2.25 (2.31) km/s; fly by Venus after 204.8 (185) days at an altitude of 3922 km with a v_∞ of 1.82 (5.58) km/s; arrive at Mercury 551.3 (663) days and 4.3 (5.8) revolutions thereafter, with maximum and average thrust acclerations of 0.36 mm/s^2 and 0.26 mm/s^2, respectively, and an ecliptic arrival v_∞ of 8.52 (0) km/s. The in-plane propellant fraction for both legs combined is 0.34, compared to Sauer's 0.28 total propellant fraction. We see that in two of the key parameters in mission design, the launch date and launch energy, the trajectories are reasonably well matched. The other parameters, while not matching as closely, do exhibit a rough correspondence, especially after making allowances for the heuristic nature of our approach, the particular characteristics of the exponential sinusoid shape, and the eccentric orbit of Mercury.

Earth - Mars - Ceres

A broad, coarse search over the launch years 1999 to 2040 with launch v_∞s between 1.50 km/s and 2.25 km/s reveals that the year 2003, the month of April in particular, has one of the higher concentrations of low arrival v_∞ trajectories. This launch date is close to that of an EMC rendezvous trajectory optimized by Sauer.[13] Thus, a more focused search is performed over the months of April and May 2003, with launch v_∞s between 1.0 km/s and 1.7 km/s. A five-day step is used in the launch date search, since the orbital periods of the bodies involved are much

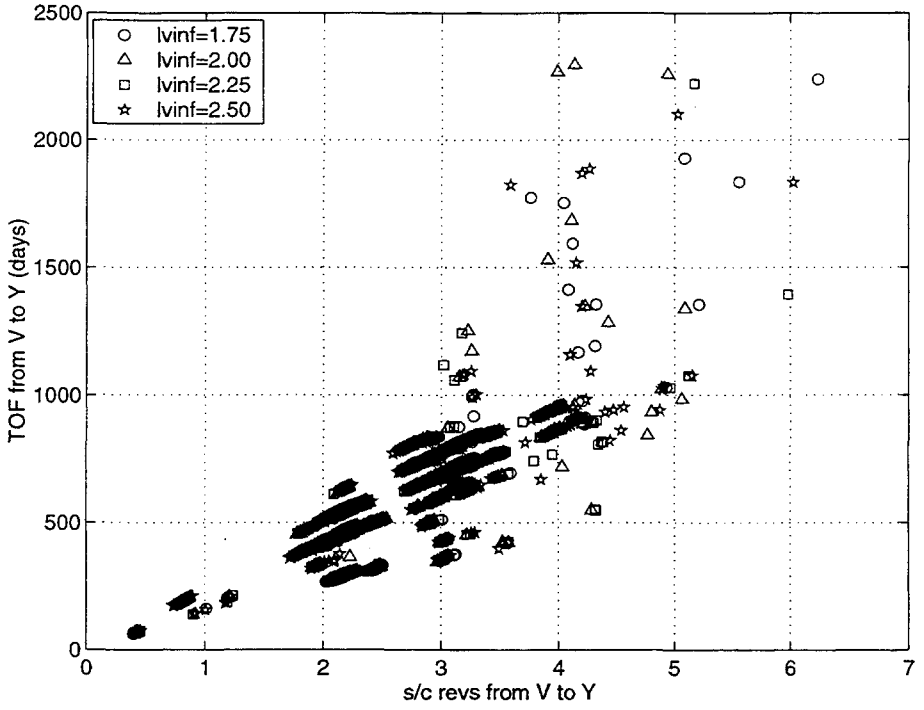

Fig. 4 Flight time from Venus to Mercury for Earth-Venus-Mercury trajectories launching between April and October 2002.

greater than five days. The ecliptic arrival v_∞ for this search is shown in Fig. 5 plotted against launch date (only v_∞s below 0.75 km/s are shown). We note a dip in the plot on May 6 (day 36). The four trajectories with the lowest ecliptic arrival v_∞s are found, upon more complete examination of the data file, to exhibit among the lowest thrust levels and propellant fractions. Details for the two most attractive of these are shown in Table 2. The data listed are launch date (L/D), launch v_∞ ($v_{\infty L}$), maximum (fmax) and average (fave) thrust accelerations for both legs, in-plane final propellant mass fraction (pmf) assuming an I_{sp} of 2000 seconds, ecliptic arrival v_∞ ($v_{\infty Aecl}$), flight times for the EM and MC legs, and total TOF. Available data are also presented in the table for the Sauer trajectory.

The second exponential sinusoid trajectory in Table 2 shows good correspondence to Sauer's optimized trajectory. The trajectory geometry is also similar: for example, the exponential sinusoid solution performs 0.56 revolutions about the sun on the EM leg and 0.67 revolutions on the MC leg, as compared with about 0.53 and 0.68 revolutions, respectively, for the optimized solution. We expect our method to provide similarly close-to-optimal solutions not only on other launch dates for the EMC case, but also for Mars gravity-assist trajectories to other asteroids.

Table 2 Exponential sinusoid Earth-Mars-Ceres trajectories and an optimized case by Sauer[13]

	ExpSin1	ExpSin2	Sauer
L/D (dd/mm/2003)	06/05	06/05	08/05
$v_{\infty L}$ (km/s)	1.40	1.60	1.37
fmax, EM (mm/s^2)	0.20	0.18	
fave, EM (mm/s^2)	0.16	0.13	
fmax, MC (mm/s^2)	0.15	0.12	
fave, MC (mm/s^2)	0.08	0.08	
pmf	0.38[a]	0.34[a]	0.28[b]
$v_{\infty Aecl}$ (km/s)	0.20	0.24	0.00
TOF EM (days)	250	271	250
TOF MC (days)	1035	862	845
TOF total (days)	1285	1133	1095

[a]Includes in-plane components only.

[b]Includes in- and out-of-plane components.

Earth - Tempel 1

We consider a transfer from Earth to the comet Tempel 1 on an exponential sinusoid, without any gravity assist. Figures 6 and 7 show results from a broad search over launch dates between June 01, 2002 and October 01, 2004 (an 856 day interval) and launch v_∞s between 2.25 km/s and 3.00 km/s. An I_{sp} of 2000 seconds is assumed, and the maximum and

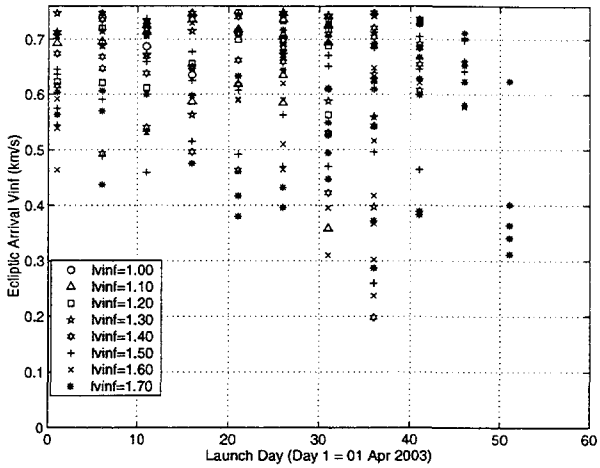

Fig. 5 Ecliptic arrival v_∞s below 0.75 km/s for Earth-Mars-Ceres trajectories launching in April and May 2003.

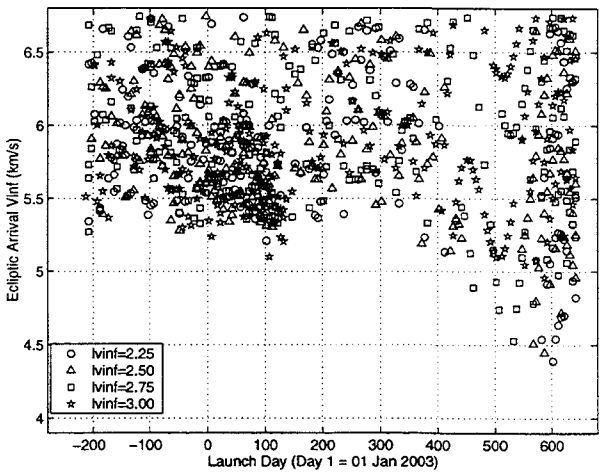

Fig. 6 Ecliptic arrival v_∞s below 6.75 km/s for Earth-Tempel 1 trajectories launching between June 2002 and October 2004.

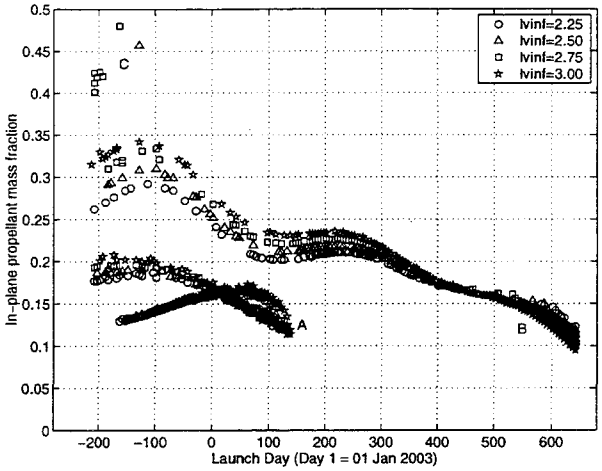

Fig. 7 In-plane propellant consumption for Earth-Tempel 1 trajectories with ecliptic arrival v_∞s below 6.75 km/s and launch between June 2002 and October 2004.

average thrust accelerations are not permitted to exceed 0.8 mm/s^2 and 0.4 mm/s^2, respectively. Only trajectories with ecliptic arrival v_∞s below 6.75 km/s are shown in the plots. We note for comparison a trajectory optimised by Sims and Flanagan[8] and Sims,[14] which launches on April 22, 2003 (day 112 in Figs. 6 and 7) with a launch v_∞ of 2.75 km/s, and has a propellant mass fraction of 0.28. This trajectory performs about 1.35 revolutions about the sun with a flight time of 2.88 years.

The somewhat large ecliptic arrival v_∞s (see Fig. 6) are due to the difficulty of matching both the flight path angle and the speed of a target in a highly elliptic orbit. However, in conjunction with these arrival v_∞s, there are very low in-plane propellant fractions (Fig. 7). As a crude means of arriving at more realistic fractions, we can consider the arrival v_∞ as a ΔV cost to be removed using the ion thruster. For a 5 km/s v_∞, this causes a propellant fraction of 0.10 to jump to 0.30, or one of 0.15 to become 0.34. (This fraction adjustment is not done in the EVY case, as its significantly larger number of revolutions about the sun makes it easier to "smear-out" existing ΔV from the thruster so as to effect a desired end condition.)

We note three distinct trajectory groupings in Fig. 7, labelled A, B and C. At the very beginning of the launch window, these groups exhibit about two, three and four revolutions, respectively, about the sun (sometimes departing heliocentrically inward from the Earth). At about -170 days, group A develops a lower branch, also with about two revolutions, but departing heliocentrically outward. Trajectories in the upper branch of group A depart inwards. As the launch date progresses, the launches of these two branches become more and more tangential, and the revolutions decrease towards one, at which point the group ends, around day 130. Just prior to this date, group A exhibits a local minimum of 5.10 km/s in the ecliptic arrival v_∞. This trajectory launches on April 17, 2003 with a launch v_∞ of 3.00 km/s, requiring an in-plane propellant mass fraction of 0.13 and an average in-plane thrust acceleration of 0.09 mm/s^2. Its time of flight is 2.01 years (0.99 revolutions about the sun) and it meets Tempel 1 when both are heliocentrically inbound. This is somewhat different from the Sims-Flanagan trajectory, which takes a lit-

tle longer and meets Tempel 1 after its perihelion passage. Such encounters are also found by STOUR-LTGA, but they have arrival v_∞s above about 9 km/s due to the shallow flight path angle and the low speed on the exponential sinusoid at the encounter point.

Trajectories in group B also exhibit a decrease in revolutions about the sun as the launch date progresses. By the end of the launch window they drop from about three revolutions to between about 0.5 and 1. The low propellant fractions and low arrival v_∞s towards the end of the launch window are attractive, but come at the price of higher thrust levels (around 0.16 mm/s^2 average thrust acceleration). This is to be expected since with fewer revolutions there is less time to build-up the required speed for rendezvous. Thus, should these higher thrust levels be available, the latter part of the launch window appears most likely to yield suitable starting points in optimization.

Conclusions

While heuristic in nature, a shape-based approach can yield readily computable, low propellant cost, low-thrust gravity-assist trajectories. In particular, using the exponential sinusoid shape, we have been able to match (approximately) the general characteristics of three propellant-optimal rendezvous trajectories reported in the literature. A good match can be found when the shape is well suited to the orbital geometries of the bodies involved, as in the case of Earth-Mars-Ceres. In other cases, such as the spiraling rendezvous to a highly elliptic target orbit, if allowances are made for the limitations imposed by the shape, our approach can still provide a rough indication of the optimal trajectory characteristics.

The exponential sinusoid shape can also be used for non-rendezvous missions, such as simple flybys or heliocentric escape. While the inclusion of coast arcs is not described in this paper, the shape-based approach is well suited to accommodating such arcs. In addition, the shape-based approach facilitates the reporting of discretized trajectory data. This data, available from our computer program, could be used as a starting guess in trajectory optimization using direct methods. Thus, we hope that our method will be of assistance to low-thrust gravity-assist mission designers, not only in the preliminary stages of design, but also in the more focused, latter stages of specific trajectory optimization.

Acknowledgments

This research has been supported in part by the Jet Propulsion Laboratory, California Institute of Technology under Contract Numbers 961211 (Steve Ogle, Contract Administrator and Dennis V. Byrnes, Technical Manager) and 1211514 (G. T. Rosalia, Contract Administrator and Dennis V. Byrnes, Technical Manager). We thank Steve Flanagan and Jon Sims, both of JPL, for their generous support and thoughtful suggestions.

References

[1]Williams, S. N., "Automated Design of Multiple Encounter Gravity-Assist Trajectories," M.S. Thesis, School of Aeronautics and Astronautics, Purdue University, West Lafayette, IN, Aug. 1990.

[2]Rinderle, E. A., "Galileo User's Guide, Mission Design System, Satellite Tour Analysis and Design Subsystem," Jet Propulsion Laboratory, JPL Publication D-263, Pasadena, CA, July 1986.

[3]Patel, M. R., "Automated Design of Delta-V Gravity-Assist Trajectories for Solar System Exploration," M.S. Thesis, School of Aeronautics and Astronautics, Purdue University, West Lafayette, IN, Aug. 1993.

[4]Staugler, A. J., "STOUR (Satellite Tour Design Program) User's Guide for the ΔV-EGA and V_∞-Leveraging Routines," Technical Report, School of Aeronautics and Astronautics, Purdue University, West Lafayette, IN, June 1996.

[5]Sims, J. A., Longuski, J. M., and Staugler, A. J., "V_∞ Leveraging for Interplanetary Missions: Multiple-Revolution Orbit Techniques," *Journal of Guidance, Control, and Dynamics*, Vol. 20, No. 3, May-June, 1997, pp. 409-415.

[6]Polk, J. E., Kakuda, R. Y., *et al.*, "Validation of the NSTAR Ion Propulsion System on the Deep Space One Mission - Overview and Initial Results," AIAA/ASME/SAE/ASEE Joint Propulsion Conference and Exhibit, AIAA Paper 99-2274, Los Angeles, CA, June 1999.

[7]Markopoulos, N., "Non-Keplerian Manifestations of the Keplerian Trajectory Equation and a Theory of Orbital Motion Under Continuous Thrust," AAS/AIAA Space Flight Mechanics Meeting, AAS Paper 95-217, Albuquerque, New Mexico, Feb. 1995.

[8]Sims, J. A. and Flanagan, S. N., "Preliminary Design of Low-Thrust Interplanetary Missions," AAS/AIAA Astrodynamics Specialist Conference, AAS Paper 99-338, Girdwood, Alaska, Aug. 1999.

[9]Kluever, C. A. "Optimal Low-Thrust Interplanetary Trajectories by Direct Method Techniques," *Journal of the Astronautical Sciences*, Vol. 45, No. 3, July-Sept. 1997, pp. 247-262.

[10]Betts, J. T. "Optimal Interplanetary Orbit Transfers by Direct Transcription," *Journal of the Astronautical*

Sciences, Vol. 42, No. 3, July-Sept. 1994, pp. 247-268.

[11]Petropoulos, A. E., Longuski, J. M., and Vinh, N. X., "Shape-Based Analytic Representations of Low-Thrust Trajectories for Gravity-Assist Applications," AAS/AIAA Astrodynamics Specialist Conference, AAS Paper 99-337, Girdwood, Alaska, Aug. 1999.

[12]Sergeyevsky, A. B. and Snyder, G. C., "Interplanetary Mission Design Handbook, Volume I, Part 3," JPL Publication 82-43, Jet Propulsion Laboratory, Pasadena, CA, Dec. 1, 1982.

[13]Sauer, C. G. "Solar Electric Performance for Medlite and Delta Class Planetary Missions," AAS/AIAA Astrodynamics Specialist Conference, AAS Paper 97-726, Sun Valley, Idaho, Aug. 4-7, 1997.

[14]Sims, J. A., "Trajectories to Comets Using Solar Electric Propulsion," AAS/AIAA Space Flight Mechanics Meeting, AAS Paper 00-134, Clearwater, Florida, Jan. 2000.